DEVELOPMENT OF A DEEP LEARNING NEURAL NETWORK MODEL FOR TRANSIENT AND SMALL SIGNAL STABILITY ASSESSMENT

John Obiajulu Onyemenam
Department of Electrical and Information Engineering,
Landmark University, Omu-Aran, Nigeria
john.obiajulu@lmu.edu.ng

Paul Kehinde Olulope
Department of Electrical and Information Engineering,
Ekiti State University, Nigeria
paulade001@yahoo.com

Nnaemeka Uchenn
Department of Electrical and Information Engineering,
Landmark University, Omu-Aran, Nigeria
okeke.uchenna@lmu.edu.ng

Yusuf Isaac Onimisi
Department of Electrical and Information Engineering,
Landmark University, Omu-Aran, Nigeria
yusuf.isaac@lmu.edu.ng

ABSTRACT

In contrast to past studies that only evaluated transient stability, this paper advocates using a deep learning neural network (DLNN) technique to assess both transient and small signal stability. The complexity of power system dynamic features has increased due to the introduction of new components like power electronics, electric vehicles, and renewable energy generation, making TSA and SSA essential considerations. Today, the stability and security of the electrical network are impacted by the growing development of renewable energy sources. Wide area monitoring systems for the electrical system have emerged, creating "big data," which has ushered in new paradigms for tackling these issues. A wide range of stakeholders are paying attention to transient stability and small signal stability issues because they have the potential to create catastrophic outages. This study's objective is to evaluate the numerous stability issues relating to the electrical system using feature selection and DLNN methodology. The 28-bus test case power system's dynamic simulations were used to provide Nigerian time-domain data. A data processing pipeline for feature selection is built using the Relief-F feature selection approach. If a system is transiently stable, the prediction model will advise the power system operator of the damping of low frequency local and interarea oscillations. The DLNN approach also provides information on the system's oscillatory dynamic response and transient stability, enabling the application of essential control measures. Calculations are made to determine the proper amount of

adjustment, the correct minimum damping ratio, and system stability under the constraints of stability and power balance. The DIgSILENT/Python tool, which is powered by an Intel Pentium core i5 2GHz CPU, is used to carry out this study. The Nigeria 28 bus system is used to test the suggested model's higher performance, and the IEEE 9 bus system is used to confirm it. The 28-bus system in Nigeria was evaluated as having an accuracy performance of 90.16 percent for TSA and 100 percent for SSA. This study evaluates and validates the strength of the proposed model.

Keywords- Small Signal stability assessment, Transient stability assessment, Deep Learning Neural Network, Long Short-Term Memory, Transient stability, Power system stability, Relief F, Recurrent Neural Network

I. INTRODUCTION

Power system stability refers to a power system's ability to recover from a disruption, reach equilibrium, and resume normal operations. Rotor angle instability brought on by synchronism loss has long been linked to the instability issue [7]. The instability problem has long been associated with rotor angle instability brought on by synchronism loss [7]. Depending on the intensity of the disturbance, rotor angle stability can also be divided into small signal and large signal stability. The ability of a power system to maintain synchronism in the face of little and major interruptions is often referred to as tiny signal stability and transient stability, respectively [2]. A collection of highly nonlinear Differential and Algebraic Equations (DAE) [2] and [7] describe the behavior of synchronous generators in respect to their related control systems, loads, renewable energy output, flexible AC transmission devices (FACTs), and the transmission network. The DAE model can be linearized all the way around the equilibrium point when a power system experiences small change. Small-signal stability is made possible by electrical torque changes in synchronous machines with the proper synchronizing and dampening torque component. The DAE model must be numerically solved for each circumstance using time domain simulations since it cannot be linearized around an operating point when a power system undergoes major changes [7]. The rotor angle of a synchronous generator may occasionally drift and oscillate if there is insufficient synchronizing and damping torque [2]. Transient instability, which also has the potential to reduce a power system's overall performance, is the main cause of power outages [4]. TSA, a type of time domain simulation, is expensive and computationally difficult, particularly for large power systems with an almost unlimited number of operating points and eventualities. The prediction model is trained using a Deep Learning technique (LSTM) and a data set for a variety of operating circumstances in order to accomplish these goals. The Long Short Term Memory (LSTM), which is trained to remember the oscillatory response of a projected stable system, progressively captures the significant weekly damped low frequency oscillation. The TSA and SSA's computational complexity is gradually decreased, increasing prediction accuracy, and this is also the case for the LSTM. The suggested model's enhanced performance is demonstrated using the Nigeria 28 Bus System, and its support by the IEEE 9 Bus system is provided.

II. TRANSIENT AND SMALL SIGNAL STABILITY OF A POWER SYSTEM

In this study, deep learning neural network approaches are used to build a prediction model for the transient and small signal stability issues in Nigeria's 28 bus system. This section explains the mathematical procedure for transient and small signal stability.

A. Transient Stability

A synchronous machine's ability to maintain synchronism in a power system in the wake of an interruption is referred to as rotor angle stability. Due to the fact that not all power system disturbances have the same effects on generation, some generators will slow down due to increased load from adaptive operation, while the remaining generators will increase their speed to maintain grid frequency. A change in the rotor's tilt with respect to the stator is brought on by an increase in generator speed [6]. The rotor alternately accelerates and decelerates continuously to maintain balance between the mechanical input torque and the electrical output torque. By engaging in this activity, the generator's ability to produce power is reduced, and the generator, prime mover, and transformers are all damaged. So, it's essential to protect the synchronous machine [8].

The dynamic reaction of a power system to disturbances is controlled by a collection of DAE, and their compact form is:

$$x = h\,(x, y) \qquad (1)$$

$$0 = g\,(x, y) \qquad (2)$$

The state as well as the algebraic variables x and y are shown. Additionally, h and g display the vectors of the relevant DAE. To obtain time-varying trajectories, the algebraic variables y, such as bus voltages and active power injections, and the state variables x, such as rotor angles and frequencies, are solved. To do this, the set of differential equations is discretized using numerical methods, such as the trapezoidal approach equation (1). At each time step (2), the created algebraic equations and the remaining algebraic equations are solved using the Newton's method. The dynamic trajectories over the simulation time window are observed to assess transient stability. This approach offers a precise evaluation of the temporary for a particular circumstance. [1].

B. Small signal stability

Insufficient oscillation Small signal stability is indicated by damping in frequency, rotor angle, or voltage stability indications. The amplitude of oscillatory activity is constant across time when damping is zero. Negative damping raises the oscillations' amplitude regardless of the initial disturbance. High damping ratios make the power system's critical mode larger and decrease oscillation behavior. This is because it is the component of the system that is least stable [7]. The smallest damping ratio can be used to test the stability of small signals. Small signal stability problems can be local or worldwide in scope. Interarea mode oscillations are larger disturbances created by a group of generating stations than local mode oscillations, which are smaller disturbances brought on by a single producing station. Power System Stabilizer (PSS) and Flexible AC Transmission System (FACTS) controllers are widely used to improve oscillation stability in multi-machine power systems. By generating additional signals to combat

oscillations in generator excitation systems, these devices [5] and [7] reduce damping. The main factor affecting how synchronous machines respond to oscillations is their electrical torque. Electrical torque is made up of two components: the Synchronizing Torque (TS), which oscillates in phase with the rotor angle deviation, and the Damping Torque (TD), which oscillates in phase with the components that affect the speed deviation. Both kinds of torques have an effect on the stability of tiny signals [5]. The set of algebraic and differential equations stated in (1) - (2) can be linearized around an equilibrium point for mild disturbances, as shown in equations (3) - (4).

$$\Delta x = A\Delta x + B\Delta y \quad (3)$$

$$0 = C\Delta x + D\Delta y \quad (4)$$

$$A = \frac{\partial h}{\partial x}, B = \frac{\partial h}{\partial x}, C = \frac{\partial h}{\partial x}, D = \frac{\partial h}{\partial x} \quad (5)$$

To investigate small signal or local stability at an equilibrium point in the presence of a slight disturbance in a power system, the linearized model in (3)–(4) is utilized. To do this, one employs the Lyapunov first technique, which entails determining the eigenvalues of the characteristic equation as follows. [3].

$$\det(A_{sys} - \square I) = 0 \quad (6)$$

Where, $A_{sys=A-B\ (D^{-1})C\ and}$ □=(□1, □2……□n)

Either real or complex estimated eigenvalues result in non-oscillatory or oscillatory responses. Additionally, conjugate pairs of complex eigenvalues are present, each of which indicates an oscillatory mode [5].

C. LSTM NETWORK FOR TSA AND SSA

The RNN variants known as LSTM networks are capable of retrieving historical data from time series data. By encoding incremental temporal domain inputs into long-lasting internal hidden states, the network learns. Recalling earlier information over time is a typical behavior. LSTMs are helpful for time-series prediction because they can remember prior inputs [7]. LSTMs interact in a variety of ways thanks to their chain-like structure and four interacting layers. LSTMs are frequently employed in voice recognition, music production, and pharmaceutical research in addition to time-series predictions [7] and [10]. LSTM is used to address the long-term dependency problems. At each point, LSTM offers the choice to read, write, or reset the sale [10]. Equation 7 displays the mathematical computations for the LSTM.

$$i_t = \sigma\left(W_{ih}h_{t-1} + W_{ix}X_t + b_i\right),$$

$$\begin{aligned}
\hat{c}_t &= \tanh(W_{\hat{c}h} h_{t-1} + W_{cx} X_t + b_c), \\
c_t &= c_{t-1} + i_t . \hat{c}_t, \\
O_t &= \sigma(W_{oh} h_{t-1} + W_{ox} X_t + b_o), \\
h_t &= O_t . \tanh(c_t),
\end{aligned} \tag{7}$$

The operator denotes the pointwise multiplication of two vectors, where ct stands for the state of the LSTM cell, and Wi, Wc, and Wo are the weights. The input gate selects what fresh information can be entered while updating the cell state, while the output gate selects what information can be output based on the cell state. The LSTM cell shown in equation 8 can be mathematically characterized as follows based on the connections:

$$\begin{aligned}
f_t &= \sigma(W_{fh} h_{t-1} + W_{fx} X_t + b_f), \\
i_t &= \sigma(W_{ih} h_{t-1} + W_{ix} X_t + b_i), \\
\hat{c}_t &= \tanh(W_{ch} h_{t-1} + W_{ix} X_t + b_{\hat{c}}), \\
c_t &= f_t . c_{t-1} + i_t . \hat{c}_t, \\
o_t &= \sigma(W_{oh} h_{t-1} + W_{ox} X_t + b_o), \\
h_t &= o_t . \tanh(c_t).
\end{aligned} \tag{8}$$

Which information from the cell state will be destroyed is decided by the forget gate. When the forget gate, ft, has a value of 1, this information is stored, and when it has a value of 0 [10], it is fully discarded. The structure of the LSTM is shown in Figure 1.

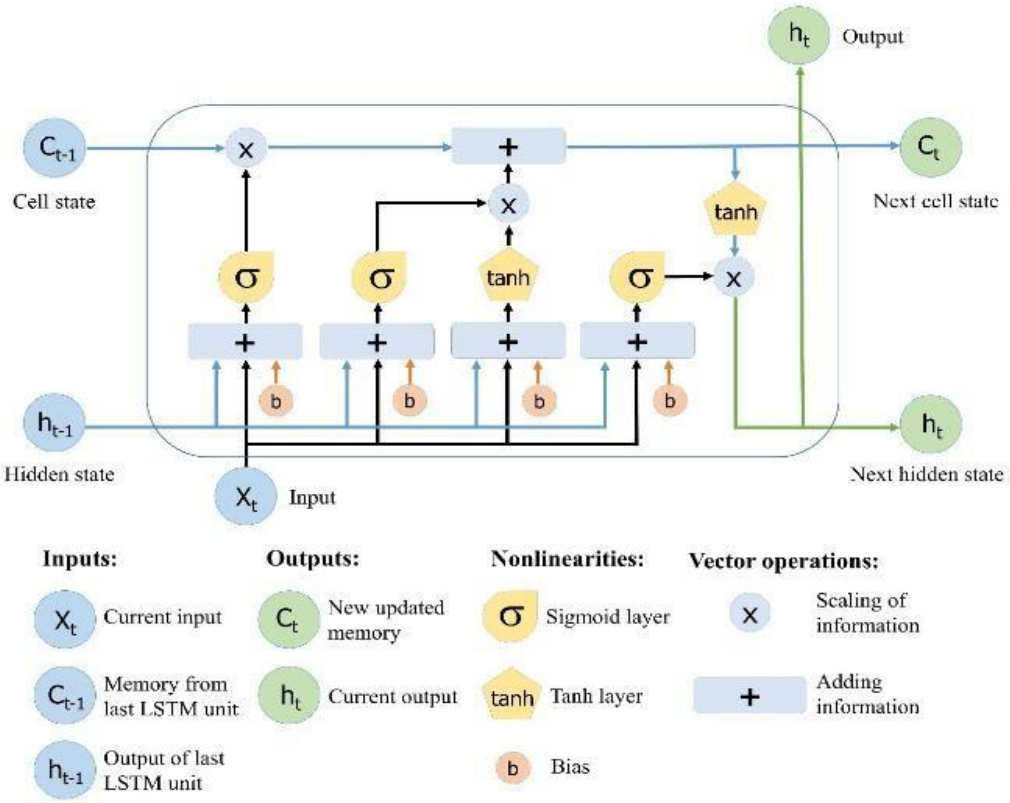

Figure 1: LSTM Network Diagram [11].

III. NETWORK STRUCTURE OF THE MODEL

In order to create a Deep learning NN for TSA and SSA, this paper builds the six-layer network model are explained below

i. Data collection: The National Control Center (NCC), Oshogbo, is where appropriate data for modeling the 28-bus Nigeria network are acquired.

ii. Using DIgSLIENT, the Nigeria 28 bus system was network modeled.

iii. Data collection for DLNN: The Relief-F technique is applied to remove unusual data from redundant ones.

iv. DLNN (LSTM): A DLNN based on LSTM is modelled using the data that is available, trained, tested, and confirmed to complete the required TSA and SSA evaluation.

v. Performance evaluation: The effectiveness of the LSTM model is then assessed using the Root Mean Squared (RMS), Specificity, Accuracy, and Precision metrics.

vi. Compare outcomes: The results are evaluated against the IEEE 9 bus system.

Figure 2, shows the proposed model for assessing Transient and Small signal stability. It is made up of two different model. The two model contains four inputs namely, voltage, rotor angle, active power and reactive power.

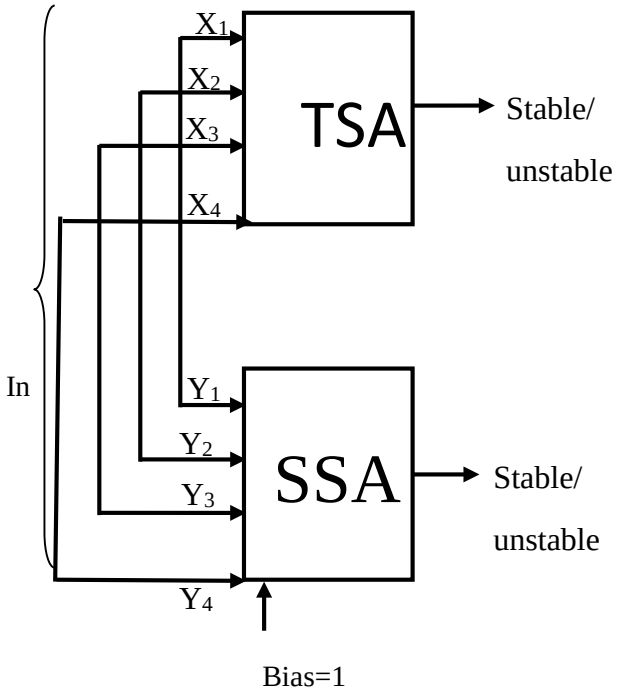

Figure 2: Schematic design model of TSA & SSA

IV. DATA PREPARATION

The National Control Center (NCC) provided the bus and transmission line data to the 330KV, 28 bus networks in Nigeria that was utilized as the case study (TCN). Figure 3 depicts the 28-bus power network, which consists of 28 buses, 9 generation stations, and 52 transmission lines. Table 1 displays the transmission line and bus data. The modeling is done in the DIgSILENT power facility. The bus bars were either PV or PQ models when it came to the transmission lines, depending on where the load and generator were positioned. The loads were lumped loads based on PQ data. Using the required information and synchronous generator characteristics, the generators were accurately modeled.

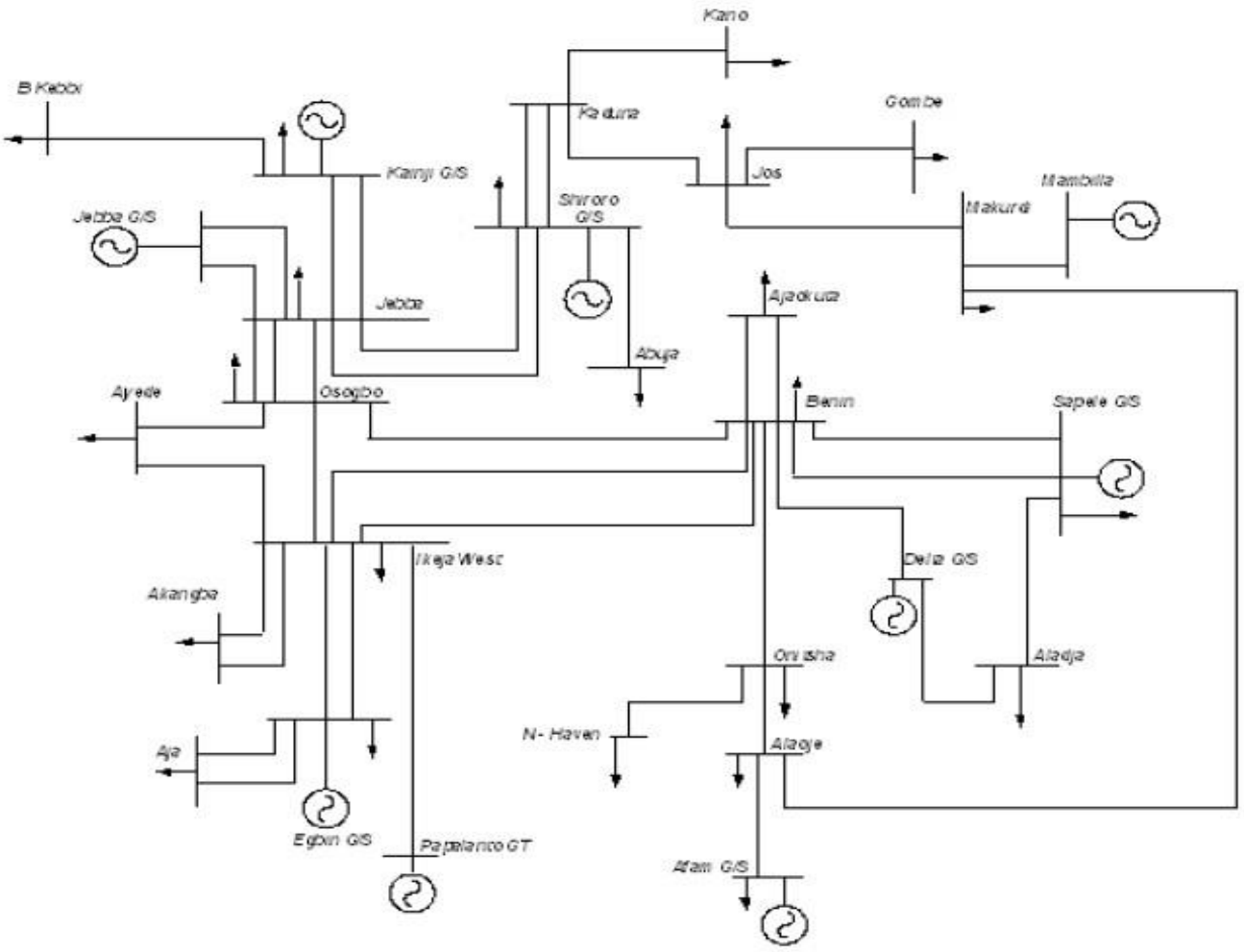

Figure 3: The Nigerian 28 bus power system [9].

Table 1: Network Data of the Nigerian 28 Bus Power System [9].

Bus Identification		Bus Loads		Transmission Lines Data			
NO	**Name**	**MW**	**MVAR**	**Bus**		**R(pu)**	**X(pu)**
1	Egbin	68.90	51.70	**FROM**	**TO**		
2	Delta 0.00	0.00	1	3	0.0006	0.0044	
3	Aja 274.40	205.80	4	5	0.0007	0.0050	
4	Akangba	244.70	258.50	1	5	0.0023	0.0176
5	Ikeja-West	633.20	474.90	5	8	0.0110	0.0828
6	Ajaokuta	13.80	10.30	5	9	0.0054	0.0405
7	Aladja 96.50	72.40	5	10	0.0099	0.0745	
8	Benin 383.30	287.50	6	8	0.0077	0.0576	
9	Ayede 275.80	206.8	2	8	0.0043	0.0317	
10	Osogbo	201.20	150.90	2	7	0.0012	0.0089
11	Afani 52.50	39.40	7	24	0.0025	0.0186	
12	Alaoji 427.00	320.20	8	14	0.0054	0.0405	
13	New-Heaven	177.90	133.40	8	10	0.0098	0.0742
14	Onitsha	184.60	138.40	8	24	0.0020	0.0148
15	B/Kebbi	114.50	85.90	9	10	0.0045	0.0340
16	Gombe	130.60	97.90	15	21	0.0122	0.0916
17	Jebba 11.00	8.20	10	17	0.0061	0.0461	
18	Jebba G	0.00	0.00	11	12	0.0010	0.0074
19	Jos 70.30	52.70	12	14	0.0060	0.0455	
20	Kaduna	193.00	144.70	13	14	0.0036	0.0272
21	Kanji 7.00	5.20	16	19	0.0118	0.0887	
22	Kano 220.60	142.90	17	18	0.0002	0.0020	
23	Shiroro	70.30	36.10	17	23	0.0095	0.0271
24	Sapele 20.60	15.40	17	21	0.0032	0.0239	
25	Abuja 110.00	89.00	19	20	0.0081	0.0609	
26	Makurdi	290.10	145.00	20	22	0.0090	0.0680
27	Mambila	0.00	0.00	20	23	0.0038	0.0284
28	Papalanto	0.00	0.00	23	25	0.0038	0.0284
				12	26	0.0071	0.0532
				19	26	0.0059	0.0443
				26	27	0.0079	0.0591

5	28	0.0016	0.0118

V. RESULT AND DISCUSSION

The test is run using the Relief-f algorithm and the LSTM. Python/DIgSLIENT is utilized to carry out this study's implementation. The Nigerian 28-bus power system for TSA and SSA is depicted in Figure 4 below using a DIgSILENT model. Data were collected from DIgSILENT for TSA and SSA purposes under various situations.

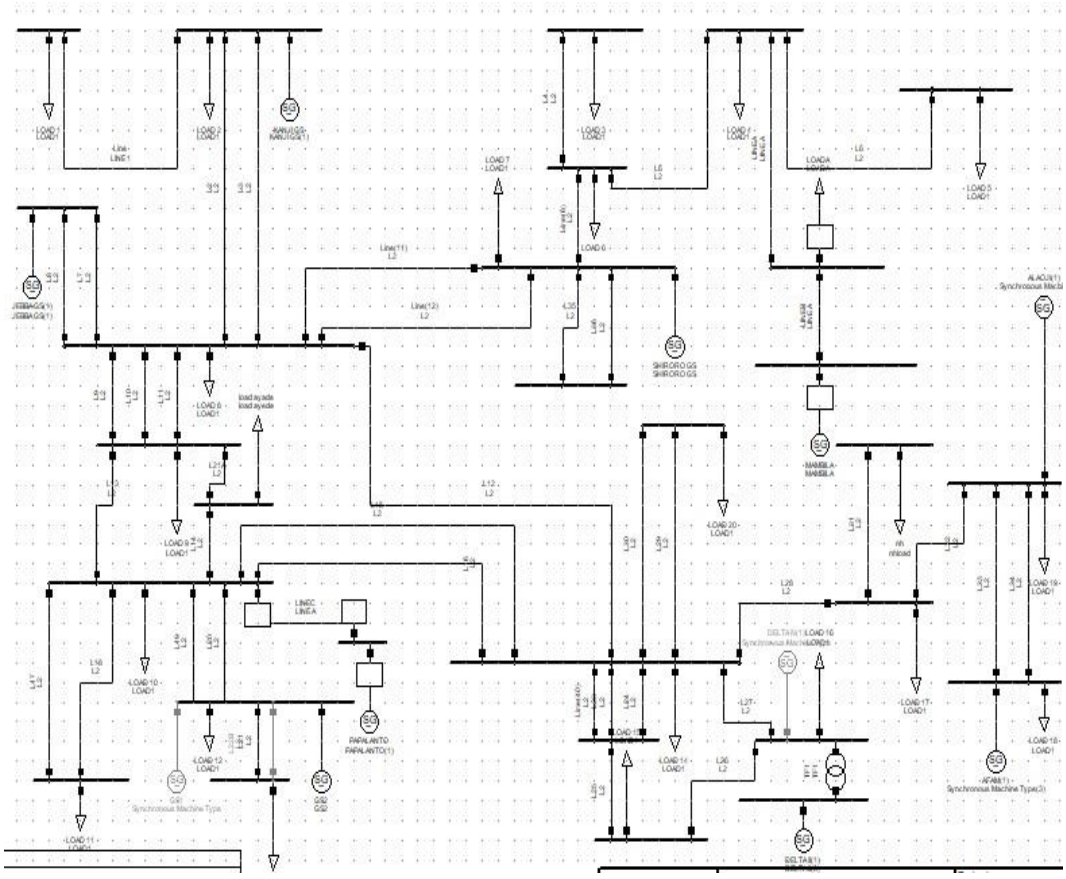

Figure 4: Modelling of Nigerian 28-Bus System

In this study the user interface gives user the privilege to load dataset, select relevant information from the huge amount of data, using the Relief-F feature selection algorithm, it helps preprocess and selects relevant subset of the data. Table 2 shows the loaded data.

Table 2: Loaded Data Nigerian 28-Bus System

V(p.u)	P(KW)	Q (KVAr	□(Ɵ)	TSA Targ	SSA Targ
0.388583	-271.618	0.454232	-63.3957	0	1
0.469965	563.2468	-306.641	97.48929	0	1
0.255932	-209.335	151.7141	-102.012	0	1
0.533196	409.5992	-385.232	58.1159	0	1
0.147646	19.65125	190.0627	-142.138	0	1
0.540542	127.6128	-338.973	17.22918	0	1
0.220532	318.4933	72.08323	176.2186	0	1
0.484492	-151.327	-180.955	-25.1795	0	1
0.370508	535.4349	-148.529	133.0507	0	1
0.366197	-274.478	26.74668	-69.1091	0	1
0.489727	539.7334	-341.938	88.36538	0	1
0.209501	-156.153	174.4907	-114.545	0	1
0.543035	309.6819	-389.185	42.17829	0	1
0.154649	150.4527	153.4337	-161.475	0	1
0.514599	-27.5849	-260.075	-5.50633	0	1
0.310105	458.6298	-49.8561	150.0938	0	1
0.403731	-252.811	-30.6135	-54.6958	0	1
0.465345	553.8266	-304.05	100.1514	0	1
0.233219	-197.255	154.0606	-105.39	0	0.135
0.54455	350.7548	-412.666	48.70475	0	0.135
0.261644	-207.228	163.5346	-100.006	1	1
0.533944	476.4872	-393.262	69.36015	1	1
0.18805	-114.21	196.6741	-121.668	1	1
0.558244	357.5287	-423.106	46.91436	1	1
0.143834	28.34095	192.7953	-144.893	1	1
0.557052	193.1078	-381.217	22.91489	1	1
0.174444	207.5377	142.6571	-169.663	1	1
0.529761	5.899559	-279.595	-2.62709	1	1

The loaded data in this study includes 81,802 instances and 6 attributes, with the targets Stable/Unstable and Eigen value. The loaded data is preprocessed and analyzed using Relief-f with DLNN. Relief-F is used to preprocess the loaded data before passing the chosen or pertinent feature to DLNN. The DLNN consists of input layers, hidden layers, and LSTM-based output layers. The ANN Fitting perspective for the data is shown in Figure 5.

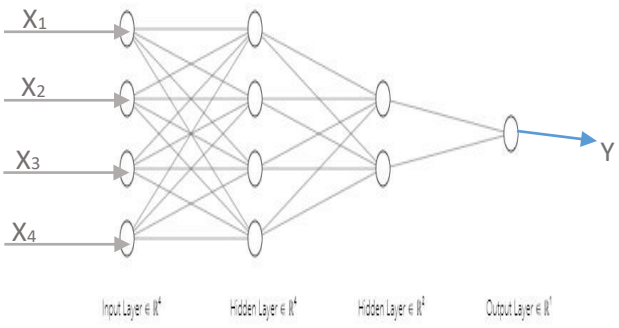

Figure 5: Fitting Layers of the Data

TSA and SSA produce either stable or unstable results. When a system is stable, the TSA denotes it as 1, and when it is unstable, it denotes it as 0. In contrast, for SSA, the system is stable or oscillatory free if the real portion of the eigenvalue is negative and the damping ratio is positive, but unstable if the real part of the eigenvalue is positive. The deep learning neural network architecture of TSA and SSA is displayed in Table 3.

Table 3: Deep learning Neural Network Data and Structure of TSA & SSA

Feature and Structure Of LSTM	**TSA AND SSA**
Number of inputs	4
Number of neurons in the hidden layer	6
Output	1 each
Training data	66560
Testing data	8256
Validation data	6273
Training algorithm	LSTM
Epoch	31
Transfer function	Relu and Sigmoid

The model confusion matrix utilized to determine the evaluation performance of the developed model, including accuracy and precision, using the DLN technique is shown in Figure 6. After 10 epochs, the system converges, and the model accuracy for TSA and SSA achieves 90.16 percent and 100 percent, respectively. Tables 4 and 5 display the model evaluation performance of the methodology.

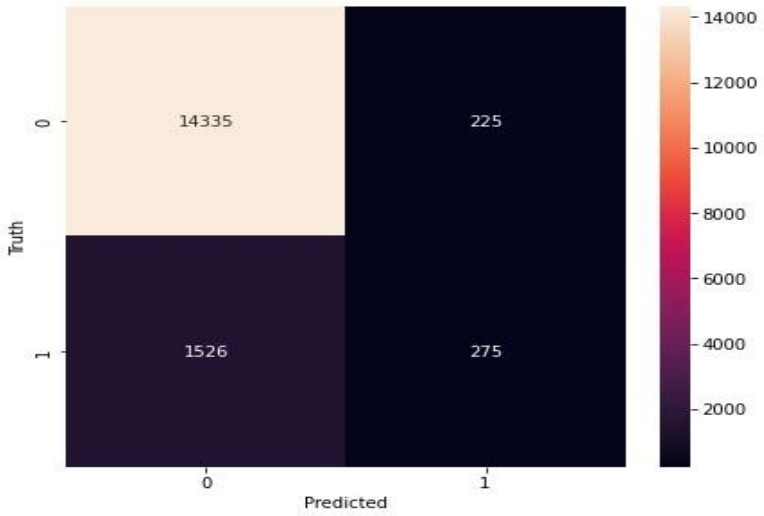

Figure 6: Confusion Matrix for the TSA Developed Model. TP=14335; TN=275; FP=225; FN=1526

Table 4: Evaluation Performance for TSA

Measure	Evaluation (%)	Derivations
Sensitivity	90.38	TRP=TP/(TP+FN)
Precision	98.45	PPV=TP/(TP+FP)
Accuracy	90.16	ACC+(TP+TN)/(P+N)

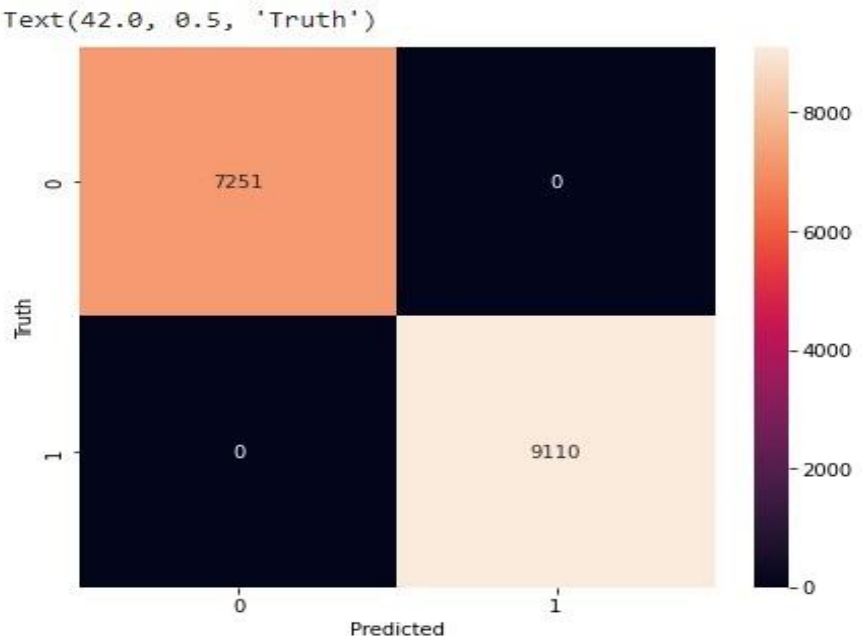

Figure 7: Confusion Matrix for the SSA Developed Model. TP=7251; TN=9110; FP=0; FN=0

Table 5: Evaluation Performance for SSA

Measure	Evaluation (%)	Derivations
Sensitivity	100	TPR=TP/(TP+FN)
Precision	100	PPV=TP/(TP+FP)
Accuracy	100	ACC=(TP+TN)/(P+N)

A. **Compare Results on IEEE 9 Bus System**

This part is illustrated in Figure 8 and uses modeling of the IEEE 9 bus system in the DIgSILENT power factory to validate the assessment outcomes from the TSA and SSA. For these systems, time-domain simulations and eigenvalue computation are performed using DIgSILENT. The generator rotor angle, voltage level, active power, and reactive power at all buses are also reported along with the oscillation modes. Additionally, a time difference of 0.3 seconds is used during the simulations' 10 second run. Table 6 displays loaded data for the IEEE 9 bus system developed and utilized for training and testing, consisting of 62,500 target values, because neural networks require a lot of data to train. For the IEEE 9-Bus system, recovered samples included 18,750 testing samples and 43,750 training samples with appropriate target values. This system exhibits oscillations with eigenvalues that are compatible with both local and inter-area modes. The simulation for SSA indicated significant eigenvalue errors. The LSTM forecasts

for this system were accurate and closely corresponded with the dynamics of the simulated oscillatory modes, in contrast to the TSA, whose LSTM predictions provided straightforward evaluation performance estimates.

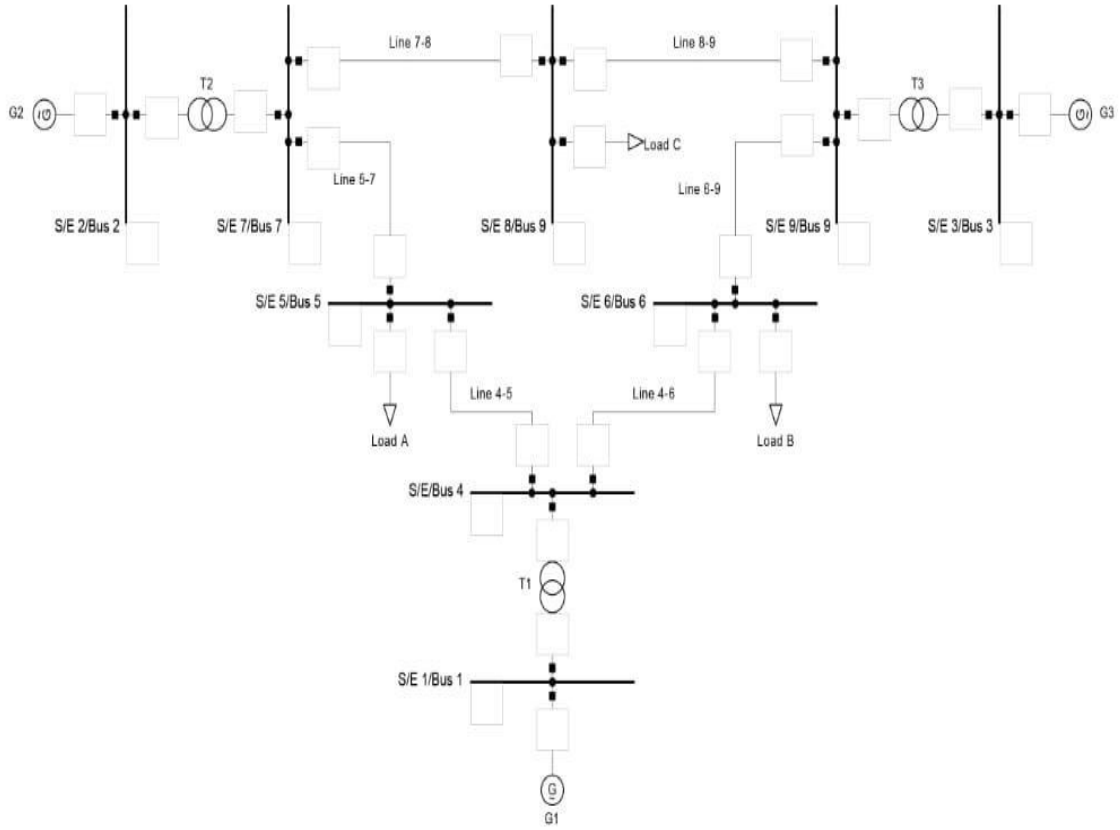

Figure 8: Modelling of IEEE 9 Bus System in DIgSILENT

Table 6: Loaded data for IEEE 9 bus system

V(p.u)	P(KW)	Q (KVAr)	□(Θ)	TSA Target	SSA Target
0.17958	-123.513	171.9536	-121.034	0	1
0.541271	191.1149	-377.243	26.03689	0	1
0.21862	312.9513	61.45572	172.7484	0	0
0.437684	-202.49	-101.296	-40.9198	0	0.982346655
0.441616	528.1544	-257.218	105.0707	0	0.982346655
0.210953	-162.216	160.9706	-109.329	0	0.10730671
0.542129	238.5471	-392.568	35.91947	0	0.10730671
0.194307	277.8757	75.5049	-179.199	0	0.085283166
0.459572	-195.994	-154.359	-34.6968	0	0.085283166
0.428978	542.6657	-250.911	109.4685	0	0
0.228289	-186.864	148.0511	-106.753	0	0
0.534469	254.3771	-375.392	36.6825	0	0
0.198982	272.5964	83.33363	179.7563	0	0
0.441242	-197.513	-114.59	-37.5489	0	0
0.445292	530.6067	-272.797	104.8101	0	0
0.194562	-150.778	160.4638	-113.223	0	0
0.542532	191.7196	-392.29	28.39765	0	0
0.227462	338.5404	33.06602	169.661	1	0.982346655
0.418274	-235.976	-78.9364	-49.4565	1	0.982346655
0.468614	509.4048	-308.579	91.10054	1	0.10730671

The TSA model confusion matrix, which was calculated using the DLNN technique to determine the evaluation performance of the developed model, including accuracy and precision, is shown in Figure 9 and Table 7. The outputs of the TSA's confusion matrix model are TP=2300, TN=5900, FP=4000, and FN=370. After 82 epochs, the system converges, and the model accuracy for TSA is 65%.

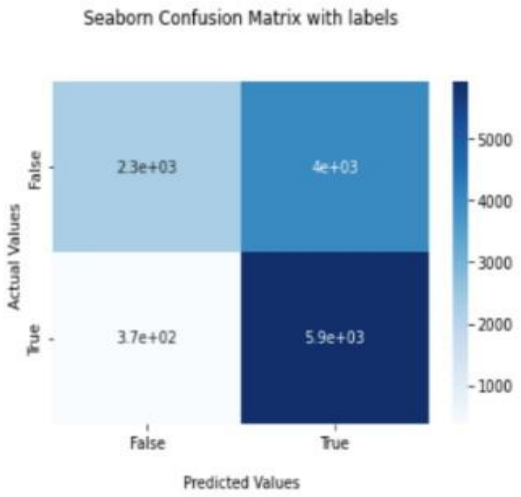

Figure 9: Confusion matrix for the TSA IEEE 9 bus system

Table 7: Evaluation Performance for TSA of IEEE 9 bus system

Measure	Evaluation (%)	Derivations
Sensitivity	94	TPR=TP/(TP+FN)
Precious	86	PPV=TP/(TP+FP)
Accuracy	65	ACC=(TP+TN)/(P+N)

Because the goal values have so many floats and so few integers, the SSA outcome is a Regression method. After 40 epochs, the system converges, producing a Mean Squared Error of 0.183 and a Root Mean Squared Error of 0.4277849927. Figure 10 depicts the Residual Distribution Curve, where the prediction is both over and under estimated because the majority of the estimated values fall between -0.5 and 0.5.

print (‘MSE: ‘ + str(mse)) print

(‘MSE: ‘ + str(rmse)) print

(‘Epochs: ‘ + str(5))

MSE: 0.183

RMSE: 0.4277849927

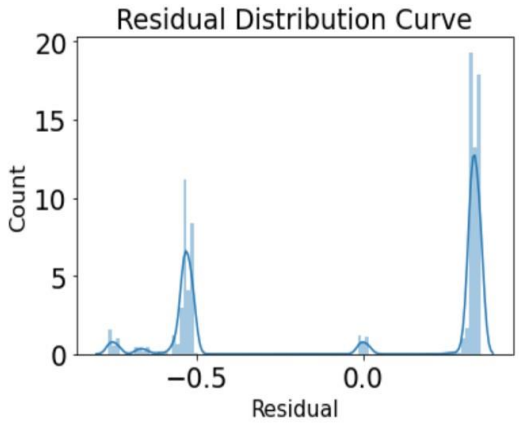

Figure 10: Residual Distribution Curve

A number of studies on TSA and SSA were compared to the outcomes utilizing different machine learning approaches. The accuracy of various methods for predicting TSA and SSA is compared in Table 8. The proposed method is tested utilizing the IEEE 58, IEEE 60, and New England 39 bus systems after being compared to CNN and LSTM in Table 8 to anticipate TSA and SSA. The MSE, RMSE, Accuracy, Sensitivity, and Precision are the primary comparing measures. The Nigeria 28 bus system has faultless assessment performance for both TSA and SSA because to the usage of LSTM to increase its accuracy, sensitivity, and precision. Because there were so many floats in the input data, TSA's accuracy was low. The accuracy of the evaluation performance when using the IEEE 9 bus system was 65%. To improve TSA accuracy in this case, random hyperparameter tweaking can be employed, although a longer training period is required. While in SSA, the MSE can be improved by using random search hyperparameter adjustment and can also be improved by adding more LSTM layers to make sure that it won't overfit the data.

Table 8: Comparison of performance with TSA and SSA methods

Related works on (TSA and SSA)	Method	Accuracy %) (	Sensitivity %) (	Precision %) (	MSE	RMSE
Nigeria 28 Bus System (proposed work)	LSTM	90.16 100	90.8 100	98.45 100	_	_
IEEE 9 Bus System (proposed work)	LSTM	65	94	86	0.183	0.42778
IEEE 50 Bus System[7].	CNN and LSTM	98.31	_	_	0.00000016	0.0004
New England 39 Bus System[7].	CNN and LSTM	94.5	_	_	0.00001024	0.0032
IEEE 68 Bus System[7].	CNN and LSTM	97.22	_	_	0.00001681	0.0041

VI. CONCLUSION

It is now simpler to convert the current power systems into a new generation of power systems with a high penetration of renewable energy and power electronics thanks to the integration of power electronics technology and renewable energy sources. This change makes it very difficult to evaluate the electrical networks' transient and small signal stability. Datadriven TSA with SSA methods establish a relationship between system operational parameters and stability status before determining stability results without the need for a power system's physical model or parameter information, in contrast to conventional time domain simulation and energy function methods. For the safe and dependable operation of electricity networks, transient stability and small signal stability are essential In order to evaluate small signal stability and transient stability, feature-based deep learning methods (LSTM) are introduced in this study. The findings of the study will benefit those who are interested in the topic by improving their understanding of LSTM in assessing transitory and tiny signal stability.

REFERENCES

[1] BIN, Z., & XUE, Y. (2019). A method to extract instantaneous features of low frequency oscillation based on trajectory section eigenvalues.
Journal of Modern Power Systems and Clean Energy, *7*(4), 753–766. https://doi.org/10.1007/s40565-019-0556-z

[2] Lim Zhu Aun, S., Bte Marsadek, M., & K. Ramasamy, A. (2017). Small Signal Stability Analysis of Grid Connected Photovoltaic. *Indonesian Journal of Electrical Engineering and Computer Science*, *6*(3), 553. https://doi.org/10.11591/ijeecs.v6.i3.pp553-562

[3] Liu, X., Ding, C., Wang, Z., & Zhou, P. (2011). Direct method to analyze small signal stability of electric power systems. *Dianli Zidonghua Shebei/Electric Power Automation Equipment*, *31*(7), 1–4.

[4] Nikolaev, N., Dimitrov, K., & Rangelov, Y. (2021). A Comprehensive Review of Small-Signal Stability and Power Oscillation Damping through Photovoltaic Inverters. *Energies*, *14*(21), 7372. https://doi.org/10.3390/en14217372

[5] Prasertwong, K., Mithulananthan, N., & Thakur, D. (2010). Understanding Low-Frequency Oscillation in Power Systems. *The International Journal of Electrical Engineering & Education*, *47*(3), 248–262. https://doi.org/10.7227/IJEEE.47.3.2

[6] Sarajcev, P., Kunac, A., Petrovic, G., & Despalatovic, M. (2022). Artificial Intelligence Techniques for Power System Transient Stability Assessment. *Energies*, *15*(2), 507. https://doi.org/10.3390/en15020507

[7] Syafiq, K. A., Younes,J. I., Mohamed, S. El., Khaled, E. (2020). A Unified Online Deep Learning Prediction Model for Small Signal and Transient Stability. IEE Transactions on Power Systems, 35(6).

[8] Krištof, V., & Mešter, M. (2017). Loss of excitation of synchronous generator. *Journal of Electrical Engineering*, *68*(1), 54–60. https://doi.org/10.1515/jee- 2017-0007

[9] Source: National Control Center (NCC), Power Holding Company of Nigerian,2012. Available at: www.nerc.gov.ng

[10] Mikolov, T., Joulin, A., Chopra, S., Mathieu, M., & Ranzato, M. 'A. (2015). Learning longer memory in recurrent neural networks. *3rd International Conference on Learning Representations, ICLR 2015 - Workshop Track Proceedings*.

[11] Ren, C., Xu, Y., & Zhang, Y. (2018). Post-disturbance Transient stability assessmentof power system towards optimal accuracy-speed tradeoff. Protection and control of Modern Power Systems, 3(1), 19. https://doi.org/10.1186/s41601-018-0091-3